Journal of Power Sources 187 (2009) 204–208

Contents lists available at ScienceDirect

Journal of Power Sources

journal homepage: www.elsevier.com/locate/jpowsour

Short communication

Electrical and microstructural characterization of two-step sintered ceria-based electrolytes☆

C.M. Lapa[a], D.P. Ferreira de Souza[a], F.M.L. Figueiredo[b], F.M.B. Marques[b,*]

[a] Department of Materials Engineering, UFSCAR, São Carlos, Brazil
[b] Ceramics and Glass Engineering Department/CICECO, University of Aveiro, 3810-193 Aveiro, Portugal

ARTICLE INFO

Article history:
Received 2 June 2008
Received in revised form 29 August 2008
Accepted 19 October 2008
Available online 28 October 2008

Keywords:
Solid electrolytes
Solid oxide fuel cells
Ceria
Sintering
Microstructure

ABSTRACT

Gadolinium-doped ceria-based materials with and without Ga-additions were prepared following several firing schedules including one peak sintering temperature (up to 1300 °C) with or without subsequent dwell at lower temperature (at 1150 °C). Sintered disks with submicrometric grain size and densifications in the order of 92% or higher, were obtained in this manner, with the final result depending slightly on the sintering profile and presence of Ga as dopant. All materials were characterized by scanning electron microscopy, X-ray diffraction and impedance spectroscopy in air, in the temperature range 200–800 °C. The grain boundary arcs were found slightly dependent on grain size and porosity but significantly on Ga-doping, due to the likely presence of large concentrations of Ga along the grain boundary region.

1. Introduction

After decades of development, the state of the art solid oxide fuel cells (SOFCs) still fail to meet the ideal performance and/or cost requirements to become fully competitive with respect to alternative classical systems known for their detrimental environmental impact. One of the major trends in SOFC development is towards reduction of the cell working temperature to enable the use of affordable stack materials.

Ceria-based electrolytes are known as promising materials for intermediate temperature SOFCs, with Gd- (GCO) and Sm-doped ceria being recognized as the materials with better conductivity within this family of compositions [1–4]. The high ionic conductivity of these materials provides a significant advantage with respect to the well established and reliable zirconia-based solid electrolytes, requiring working temperatures in the order of 1000 °C. Attempts to improve the performance of ceria-based materials include compositional effects, namely the role of dopants and co-doping [5–13], and microstructural effects with emphasis on the role of grain size, including nanosized materials [14,15].

Strategies to obtain nanostructured ceria-based ceramics were mostly based on sintering additives that lower densification temperatures. One particular example is the exploitation of CoO additions, able to produce dense ceramics at sintering temperatures a few hundred centigrade lower that the corresponding Co-free materials. However, this approach is responsible for an undesirable increase in the electronic conductivity [5,6].

Recent reports on the effects of small Ga_2O_3 additions on the optimization of the sintering behavior of ceria-based ceramics seem rather promising, although little information is available on the impact of such additions on the electrical transport properties of these materials [9–13].

As an alternative route to obtain nanostructured materials, two-step sintering profiles were found effective in preventing grain growth. The idea behind this approach is to exploit the differences in kinetics between grain growth and densification [14].

Lowering the sintering temperature of ceria-based electrolytes might also favor the possibility of co-sintering electrolyte and electrodes, one of the interesting solutions often tested in SOFC development.

In the present work these two parallel approaches were combined and exploited aiming at an assessment of both routes to obtain dense GCO-based electrolytes at relatively low temperature. A classical chemical route was adopted in order to obtain nanosized GCO powders as starting materials. These powders, with and without Ga-additions, were then sintered following a two-step sintering profile including several peak temperatures with or without

☆ This paper was presented at Hyceltec, the 1st Iberian Symposium on Fuel Cells, Hydrogen and Advanced Batteries, Bilbao, Spain, 2008 July 1–4.

* Corresponding author. Tel.: +351 234370269; fax: +351 234425300.
E-mail address: fmarques@ua.pt (F.M.B. Marques).

0378-7753/$ – see front matter © 2008 Elsevier B.V. All rights reserved.
doi:10.1016/j.jpowsour.2008.10.071

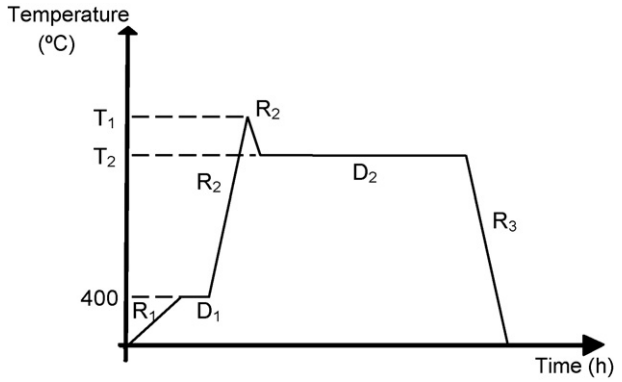

Fig. 1. Typical two-step sintering profile: T_1 – peak sintering temperature; T_2 – dwell temperature; R_1 (3.3 °C/min), R_2 (13.3 °C/min) and R_3 (16.7 °C/min) – heating/cooling rates; D_1 (0.5 h) and D_2 – dwell time (10 h).

subsequent annealing at lower temperature, to try to establish a correlation between composition, sintering conditions, microstructure and electrical performance.

2. Experimental

Gadolinia-doped ceria nanopowders (with 20 mol% dopant – GCO) were prepared by an organic synthesis route (citrate based process). Nitrates of the cations were stoichiometrically mixed with adequate amounts of citric acid and one network former (hydroxyethyl cellulose) in distilled water. After 24 h the gel was dried and the as-formed fine powder was ball-milled (dry conditions) and calcined at 450 °C. The precursor nanopowder was obtained after milling again for 6 h. Sintered bodies with small Ga_2O_3 additions (0.5 mol%) were also obtained after intimate mixing of precursors. This doping level was adopted for being identified as ideal to enhance the densification of GCO [10,12].

The calcined powders were characterized by X-ray diffraction (XRD) and transmission electron microscopy (TEM). The cubic lattice parameter was estimated after indexing the powder XRD patterns and simple fit of the peak positions. The temperature profiles, including peak sintering temperature (in the range 1250–1300 °C), dwell temperature (1150 °C), and time (0 or 10 h), at fixed heating/cooling rates, were varied in order to maximize the densification while retaining a small grain size. One typical sintering profile, depicting all parameters with influence on the final result, is shown in Fig. 1.

The sintered bodies were characterized by scanning electron microscopy (SEM) and energy-dispersive X-ray spectroscopy (EDS), both on fracture and polished and thermally etched surfaces. The electrical characterization was performed by impedance spectroscopy (frequency range 5 Hz–10 MHz, 0.5 V signal amplitude) in air (300 °C up to 1000 °C), after electroding the samples with porous Pt-electrodes. The impedance spectra were well-fitted (ZView, version 2.6, Scribner Associates) to a classical equivalent circuit consisting of two RQ parallel circuits in series (with R being a resistance and Q a constant phase angle element), for the bulk and grain boundary contributions. Maximum fitting errors for resistance estimates were 1% for Ga-doped samples and 8% for Ga-free samples.

3. Results

3.1. Microstructural and structural characterization

Observation by TEM of GCO powders calcined at 450 °C (Fig. 2) showed the presence of agglomerates consisting of powders with an individual grain size between 5 and 10 nm.

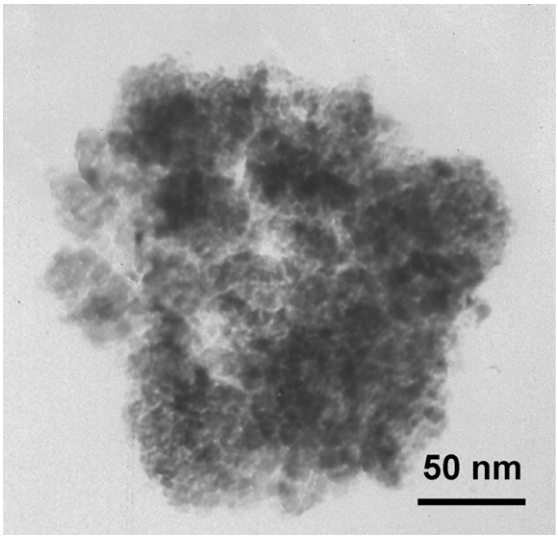

Fig. 2. TEM micrograph of GCO powders calcined at 450 °C.

The impact of Ga-additions and firing schedules on the GCO XRD pattern is shown in Fig. 3. While there is no evidence for the presence of any secondary phase after Ga-doping, a slight shift in the position of peaks at large values of 2θ is clearly noticed. This effect is expected as the result of formation of a solid solution with one cation with (smaller) different ionic radius, in substitutional position with respect to the host cation. The estimated lattice parameters for Ga-doped samples sintered at 1250/1150 and 1300/1150 °C (peak temperature/dwell temperature–10 h) were 5.412 and 5.410 Å, respectively, smaller than the corresponding value for Ga-free GCO (5.414 Å). This lattice contraction with Ga-additions was already mentioned in the literature and used to try to estimate the solubility limit of Ga in GCO [11].

The shift in the position of the high angle peaks is also slightly dependent on the firing schedule, being larger in the case of higher firing temperatures and smaller for samples annealed or sintered at lower firing temperatures. This observation suggests that formation of one fully homogeneous solid solution might not be reached with low temperature sintering conditions or after low temperature annealing, as a consequence of temperature dependent solubility of Ga in the ceria lattice. It may also suggest that sample equilibration with air was not fully achieved with fast cooling, with freezing

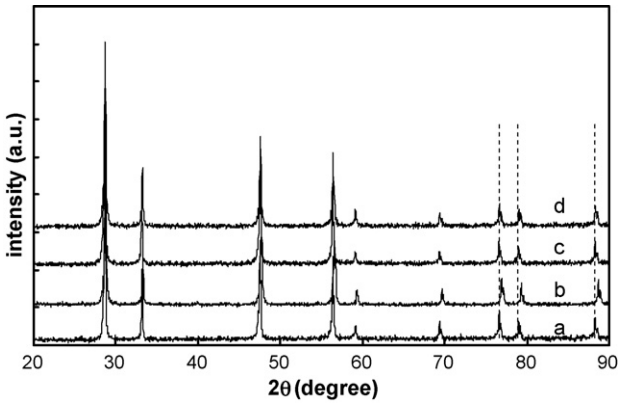

Fig. 3. XRD patterns of Ga-free GCO sintered at 1500 °C (a), and Ga-doped GCO sintered at a peak temperature of 1300 °C without dwell time (b), and sintered at a peak temperature of 1300 °C (c) and 1250 °C (d) both with a dwell time of 10 h at 1150 °C. Dashed lines highlight the slight shift in position of peaks at high angles.

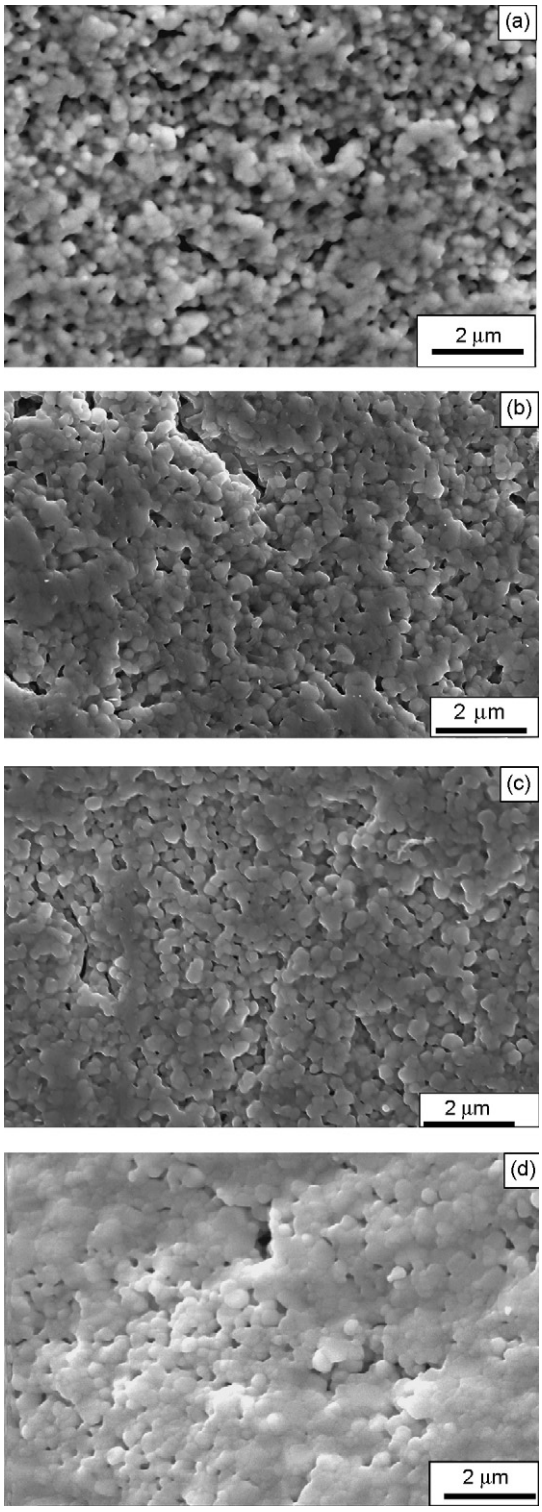

Fig. 4. SEM images of fractured GCO samples sintered at peak temperatures of 1250 (a), 1280 (b) and 1300 °C (c) all without dwell time, and sintered at a peak temperature of 1300 °C with a dwell time of 10 h at 1150 °C (d).

of some trivalent cerium and additional oxygen vacancies formed at high temperature.

Observation of microstructures of pure GCO samples, shown in Fig. 4, suggests a significant role both for the peak sintering temperature and for the dwell time. With increasing values of peak sintering temperature the densification increases, while the dwell time at relatively low temperature (1150 °C) still enhances this effect. Densities, determined from the samples geometry and weight, are shown in Table 1 to confirm the above comments. In general, the grain size increases with increasing peak temperature, while the dwell time at lower temperature has a marginal effect on grain size. In all cases the sintered samples exhibit a clearly submicrometric grain size.

Table 1
Sintering conditions and density of GCO-samples obtained following the two-step sintering process described in Fig. 1.

Composition	Sintering conditions (°C)		Density ($g\,cm^{-3}$)
	T_1 (peak temperature)	T_2 (dwell temperature)	
GCO	1250	No	6.33
GCO	1280	No	6.30
GCO	1300	No	6.56
GCO	1250	1150	6.61
GCO	1300	1150	6.71
Ga-doped GCO	1300	No	6.64
Ga-doped GCO	1250	1150	6.55
Ga-doped GCO	1300	1150	6.64

The apparently positive impact of Ga-additions on densification is shown in Fig. 5. Polishing and thermal etching masked to a certain extent the effective result. The impact in densification with respect to the corresponding Ga-free samples is marginal, in agreement with the measured density values (Table 1). However, only small closed pores can be identified in all cases, with the average grain size again clearly smaller than 1 μm, increasing slightly with increasing peak sintering temperature. The claimed positive effect of Ga-additions in the densification of conventional GCO-based powders [10–13] could not be fully confirmed in the case of nanopowders. In fact, the level of segregation of Ga along the grain boundaries, at constant overall dopant level, should be influenced by the size of grains. Consequently, the range of effective Ga-dopant levels with impact on densification is expected to shift with grain size. With the submicrometric grains obtained in this work, the results indeed deviated with respect to previous attempts with coarser grain sizes [10–13]. Evidence for Ga segregation was found in the impedance spectroscopy data detailed in the following section.

3.2. Impedance spectroscopy

Plots of the imaginary part of impedance versus the real part (corrected for the cell/electrode dimensions) are presented in Fig. 6. Two sets of samples were selected to highlight trends related to the role of major parameters exploited in this work (peak sintering temperature, dwell time and composition). In general, at low temperature, these plots show the usual features of solid electrolytes, with one high frequency arc, ascribed to the bulk grain contribution, one intermediate frequency arc, ascribed to the grain boundary contribution, and a low frequency arc related to the electrode process. The latter will be neglected in the following discussion. Also, due to the presence of significant porosity in some samples, the intermediate frequency arc is certainly influenced by the blocking role of this microstructural feature, as previously shown in the literature [16]. However, for the sake of simplicity, this arc will be simply referred to as grain boundary arc.

The role of the sintering profile in Ga-free samples is depicted in Fig. 6(a). With increasing peak sintering temperature, the overall impedance decreases, mostly due to a decreasing role of the intermediate frequency arc. This is coherent with common trends as the peak sintering temperature is also responsible for a slight increase in grain size and densification. The decreasing role of grain bound-

aries can be understood as a consequence of a decreasing value of interfacial surface area per unit volume with increasing grain size.

In Fig. 6(a) the role of the dwell time is also evidenced. While the impact of the dwell time on grain growth is rather small (Fig. 3), there is a slight overall improvement in densification (Table 1). Both effects are coherent with the decreasing magnitude of the intermediate frequency response. In fact, the blocking role of porosity with respect to charge transport is obviously smaller for samples with higher densification. As the impact of this effect is also noticed at intermediate frequencies, this trend can be explained in a comprehensive manner.

The role of the peak sintering temperature and dwell time in the sintering process and electrical performance of Ga-doped samples is also shown in Fig. 6(b). Again, as a general trend, with more intensive and extended sintering profiles, the overall impedance decreases.

Comparison of spectra shown in Figs. 6(a) and (b) puts into evidence the role of Ga-doping. In general, and with the exception of Ga-doped GCO ceramics sintered at 1250/1150 °C (peak/dwell), the high frequency arcs are within the same order of magnitude, with a slight advantage for the bulk conductivity of Ga-doped samples. However, the intermediate frequency arcs show remarkable differences in magnitude between Ga-free and Ga-doped samples, with clear advantage for pure GCO. The abnormal bulk effect noticed for Ga-doped GCO ceramics sintered at 1250/1150 °C is somewhat unexpected and may suggest a Ga–Gd interaction with consequences on the tendency to oxygen vacancy ordering, as recently suggested [17]. The marginal impact of Ga-additions on the bulk transport properties of the samples sintered at 1300 °C is probably related to the overall low concentration of dopant. The same type of situation and consequences were previously noticed in Ti-doped YSZ (yttria stabilized zirconia), where a drop in bulk conductivity was only observed at high concentrations of Ti-additions (>5 mol%) [18].

The effect of Ga-additions is clearly observed in the case of grain boundaries. The enhanced magnitude of all grain boundary arcs with respect to Ga-free samples suggests the presence of Ga-rich grain boundaries with blocking characteristics. This means that the potential beneficial effect of Ga-doping in the densification of these materials has a parallel detrimental effect on the transport properties of these materials, at least when sintered at low temperature, with relevance in the low-intermediate temperature range where grain boundaries play a significant role. To our knowledge this is the first report on the impact of Ga-additions on the transport properties of materials processed in this manner.

One final comment on the processing route adopted. For Ga-free samples, the overall performance of these materials prepared by combination of a chemical route and a two-step sintering process showed no real benefit with respect to standard materials, as well as any relevant grain size effect. In fact, the role of grain size on the transport properties is clearly within classical trends observed in polycrystalline ceramics with grain size in the order of 1 μm and higher. In this case, although showing submicrometric grain size, nanosize effects are clearly absent due to the relatively large grain dimensions. However, the densification levels reached confirm the

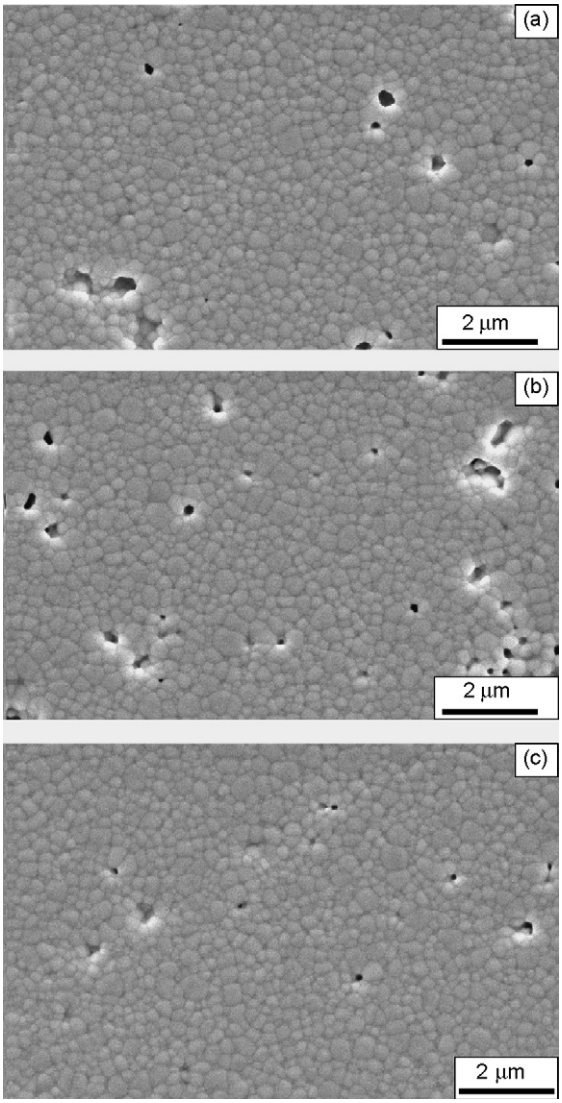

Fig. 5. SEM images of polished and thermally etched Ga-doped GCO samples sintered at peak temperatures of 1300 °C without dwell time (a), and sintered at peak temperatures of 1300 °C (b) and 1250 °C (c), both with a dwell at 1150 °C.

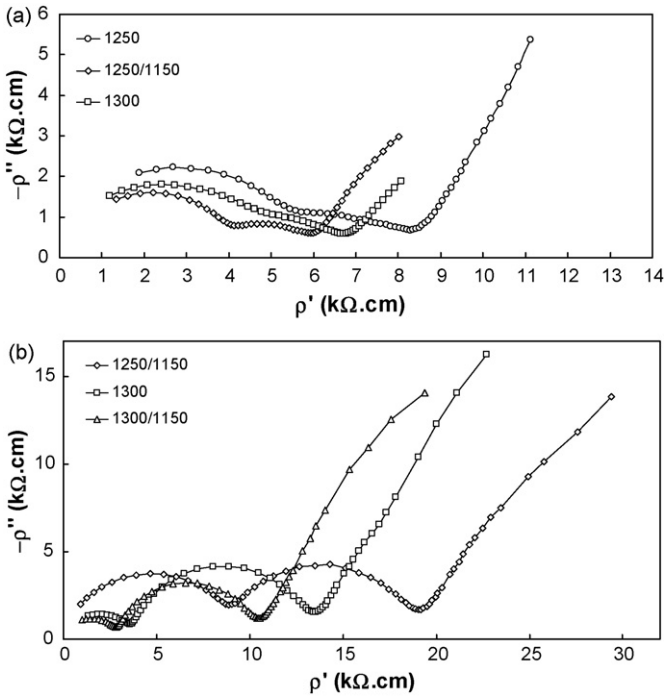

Fig. 6. Impedance spectra obtained at 300 °C, in air, of GCO samples submitted to several sintering profiles: (a) GCO samples submitted to a peak sintering step with or without subsequent dwell and (b) Ga-doped GCO samples submitted to a peak sintering step with or without subsequent dwell. In the figure inset, the peak and dwell temperatures are shown (peak/dwell, in °C).

potential of this approach for the production of these materials at relatively low sintering temperatures.

4. Conclusions

Results showed that relatively dense Ga-free ceramics (about 92% of theoretical density) with submicrometric grain size could be obtained using combinations of peak sintering temperatures at or below 1300 °C, and subsequent lower temperature annealing, following the adopted two-step sintering route. Ga-additions provided a marginal improvement in the densification of these materials.

Impedance spectroscopy data could be conveniently related to the samples microstructure and composition, with the intermediate frequency response strongly dependent on grain size, porosity and Ga-doping. Ga-additions provided a noticeable increase in the electrical resistance mostly due to an enhanced intermediate frequency contribution ascribed to the formation of Ga-rich grain boundaries. The tendency to a slightly positive effect of Ga co-doping on the bulk electrical transport parameters deserves further attention.

Acknowledgement

Financial support from CAPES and CNPq (Brazil), FCT (Portugal) and the NoE FAME (CEC, Brussels) is greatly appreciated.

References

[1] H. Inaba, H. Tagawa, Solid State Ionics 83 (1996) 1–16.
[2] B.C.H. Steele, Solid State Ionics 129 (2000) 95–110.
[3] V.V. Kharton, F.M. Figueiredo, L. Navarro, E.N. Naumovich, A.V. Kovalevsky, A.A. Yaremchenko, A.P. Viskup, A. Carneiro, F.M.B. Marques, J.R. Frade, J. Mater. Sci. 36 (5) (2001) 1105–1117.
[4] V.V. Kharton, F.M.B. Marques, A. Atkinson, Solid State Ionics 174 (2004) 135–149.
[5] C.M. Kleinlogel, L.J. Gauckler, J. Electroceram. 5 (2000) 231–243.
[6] C.M. Kleinlogel, L.J. Gauckler, Solid State Ionics 135 (2000) 567–573.
[7] T. Zhang, Z. Zeng, H. Huang, P. Hing, J. Kilner, Mater. Lett. 57 (2002) 124–129.
[8] T.S. Zhang, J. Ma, L.B. Kong, S.H. Chan, P. Hing, J.A. Kilner, Solid State Ionics 167 (2004) 203–207.
[9] H. Yoshida, K. Miura, J. Fujita, T. Inagaki, J. Am. Ceram. Soc. 82 (1999) 219–221.
[10] J.S. Lee, K.H. Choi, B.K. Ryu, B.C. Shin, I.S. Kim, J. Mater. Sci. 40 (2005) 1153–1158.
[11] J.S. Lee, K.H. Choi, B.K. Ryu, B.C. Shin, I.S. Kim, Mater. Res. Bull. 39 (2004) 2025–2033.
[12] J.S. Lee, K.H. Choi, M.W. Park, D.J. Kwak, K.H. Shin, C.W. Shin, J. Mater. Sci. 41 (2006) 7983–7988.
[13] J.S. Lee, J. Electroceram. 17 (2006) 709–711.
[14] L.W. Chen, X.H. Wang, Nature 404 (2000) 168–171.
[15] E. Ruiz-Trejo, A. Benítez-Rico, S. Gómez-Reynoso, M. Angeles-Rosas, J. Electrochem. Soc. 154 (4) (2007) A258–A262.
[16] M.C. Steil, F. Thévenot, M. Kleitz, J. Electrochem. Soc. 144 (1997) 390–396.
[17] D.R. Ou, T. Mori, F. Ye, J. Zou, G. Auchterlonie, J. Drennan Phys. Rev. B 77 (2008), doi:10.1103/PhysRevB.77.024108, 024108.
[18] L.S.M. Traqueia, T. Pagnier, F.M.B. Marques, J. Eur. Ceram. Soc. 17 (1997) 1019–1026.